ELSEVIER

Journal of Chromatography A, 888 (2000) 175–196

JOURNAL OF CHROMATOGRAPHY A

www.elsevier.com/locate/chroma

Surface characterization of industrial fibers with inverse gas chromatography

Arian van Asten, Nico van Veenendaal*, Sander Koster

General Analytical and Environmental Chemistry Department, Akzo Nobel Central Research, PO Box 9300, 6800 SB, Arnhem, The Netherlands

Received 19 October 1999; received in revised form 17 April 2000; accepted 19 April 2000

Abstract

Inverse gas chromatography (IGC) was applied for the determination of the surface characteristics of Tenax carbon fibers and Akzo Nobel Twaron fibers. Furthermore, IGC procedures for the determination of dispersive and acid–base interactions were validated. The data show that too high values for the dispersive component of the surface energy are obtained when the adsorption area occupied by a single adsorbed *n*-alkane molecule is estimated from parameters of the corresponding liquid. Comparable values are obtained when the Doris–Gray methodology (area per methylene unit) or measured probe areas are employed. For the fibers studied in this work meaningful Gibbs energy values of the acid–base interaction were only obtained with the polarizability approach. When the dispersive interaction of the polar probes with the fiber surface was scaled to the *n*-alkane interaction via surface tension, the boiling point, or the vapor pressure of the probes often negative acid–base interaction energies were found. From the temperature dependence of the Gibbs energy, the enthalpy of the acid–base interactions of various probes with the carbon and Twaron aramid fibers was determined. However, from these enthalpy values no meaningful acid–base surface parameters could be obtained. Generally, the limited accuracy with which these parameters can be obtained make the usefulness of this procedure questionable. Also the Gibbs energy data of acid–base interaction can provide a qualitative basis to classify the acidity–basicity of the fiber surface. This latter approach requires only a limited data set and is sufficiently rapid to enable the use of IGC as a screening tool for fibers at a production site. For several polar probes significant concentration effects on carbon fibers were observed. At very low probe loadings the interaction with the fiber surface suddenly increases. This effect is caused by the heterogeneity of the interaction energy of the active sites at the surface. A simple procedure to measure the adsorption isotherm at infinite dilution was developed. The determination of the concentration dependence of the interaction of an *n*-alkane, an acidic and a basic probe was incorporated in the IGC screening procedure of carbon fibers to monitor this heterogeneity.

Keywords: Inverse gas chromatography; Surface characteristics; Fibers; Tenax; Twaron

1. Introduction

With inverse gas chromatography (IGC) non-volatile material, either in the liquid or solid state, can be studied by applying it as a stationary phase in a gas chromatographic (GC) column. The interaction of

*Corresponding author. Fax: +31-26-366-5280.

E-mail address: nico.vanveenendaal@akzonobel.com (N. van Veenendaal).

0021-9673/00/$ – see front matter
PII: S0021-9673(00)00487-8

volatile probes (injected onto the column according to standard GC procedures) with the stationary phase reflects the physical and chemical state of the material under investigation. After the introduction of IGC in 1967 [1] and subsequent theoretical developments [2], the application of IGC in the material sciences has grown rapidly. IGC has been used for the characterization of polymers, copolymers, polymer blends, biopolymers, industrial fibers, wood and pulp fibers, composites, coatings, pigments, catalysts, unmodified and deactivated silica capillaries and particles, glass beads, coal, chemicals and steel tubing. Although it is outside the scope of this work to provide literature references on each type of IGC application, information on the IGC characterization of many of the above listed materials can be found in Refs. [3] and [4]. IGC is a popular tool for material characterization because it is a versatile, robust, user friendly, and inexpensive technique. The use of a standard GC set-up ensures data collection over a wide temperature range. This accounts for the versatility of IGC, together with the variety of volatile probes that are available and the possibility to vary the probe concentration.

The surface characteristics of industrial, textile, and natural fibers usually play an important role in the technological application of these materials. Especially in composites, the chemical nature of the fiber surface is of importance as it determines to a large extent the degree of adhesion of the reinforcing fiber to the polymer matrix [5–12]. (It should be noted that the correlation of the strength of adhesion and the ''overall toughness'' of the composite can be less straightforward [13]). To improve adhesion characteristics the surface of fibers are frequently modified prior to application. The surface of the carbon fibers is activated via (plasma [14,15]) oxidation [5,7,8,16] or sizing [5,7,8,16] (the application of oil, surfactant or a polymer film to facilitate fiber processing). The surface modification of Kevlar fibers by PDMS coating, grafting, and chemical etching has also been reported [13]. The surface characteristics of cellulose and lignocellulose fibers have been altered by plasma [11] and corona [17] treatment, grafting [18], bleaching [19], and extraction [20]. Finally, surface modification of glass fibers by means of grafting has been described in the literature [9,10,21,22].

To understand the effects of the fiber surface treatment on the final characteristics of fibers and composites, surface characterization tools are required. Physio–chemical techniques as wetting measurements (either by contact angle determination or the Wilhelmy method) [5,7,8,13,18,19,23,24], X-ray photoelectron spectroscopy (XPS) [8,9,11,12,14,16–19,24], titration [14], microcalorimetry [9,12], zeta-potential measurements [8,14–16,24], scanning electron microscopy (SEM) [9,11], fourier transform infra-red spectroscopy (FTIR) [9] and IGC have been used to obtain detailed information on fiber surfaces. Because of its merits, as outlined above, IGC has frequently been applied for fiber surface characterization. IGC studies of carbon [5–8,14,16,25], glass [10,21,22], textile [24], nylon [23], and cellulose based fibers [11,17–20,26–28] have appeared in the literature. In this work the IGC characterization of modified and unmodified Tenax carbon fibers and Akzo Nobel Twaron fibers is reported. Furthermore, the various methods described in the literature to extract meaningful thermodynamic parameters from IGC data are evaluated.

2. Theory

The general theoretical framework for the thermodynamic description of dispersive and specific or so-called acid–base interactions of probe molecules at a surface has been given by many authors (e.g., [29–31]) In this section this framework will be summarized to clarify the discussion given in Section 4.

2.1. Determination of the dispersive component of the surface free energy

In general, the net retention volume, V_n, of a probe is directly related to the thermodynamic interaction with the surface. The net retention volume can accurately be determined from the flow-rate at the column exit, F_0, and the residence times of an unretained compound (usually methane), t_0, and of the probe, t_r. If a soap bubble flow meter is used and the gas compressibility is accounted for, V_n is obtained from the measured parameters given above by:

$$V_n = jF_0 \cdot (t_r - t_0) \cdot \frac{T_c}{T_f} \cdot \left(\frac{p_0 - P_{H_2O}}{p_0} \right) \quad (1)$$

where j is the well known James–Martin correction factor for gas compressibility, T_c and T_f are the temperature at the column and flow meter, p_0 is the pressure at the column outlet and P_{H_2O} is the water vapor pressure at T_f.

Normally, IGC fiber columns have a very low flow resistance which makes gas compressibility effects negligible (i.e., $j=1$). If IGC measurements are conducted at infinite probe dilution to prevent probe–probe interactions, the molar free energy of adsorption, ΔG_m^{ads}, is related to V_n according to:

$$\Delta G_m^{ads} = -RT \cdot \ln(V_n) + C \quad (2)$$

where R is the gas constant, T is the temperature and the constant C depends on the choice of the reference state:

$$C = -RT \cdot \ln\left(\frac{A\pi}{p_{s,g}} \right) \quad (3)$$

where $p_{s,g}$ is the probe vapor pressure in the standard gaseous state, π is the surface pressure and A is the specific surface area of the stationary phase.

Work by Fowkes [32–34] on surface adsorption has led to the conclusion that the work of adhesion, W_a, between a probe and a solid is mainly governed by dispersive (i.e. London) and acid–base (including hydrogen-bonding) interactions. Generally, these interactions are considered to be independent and, therefore, additive:

$$W_a = W_a^D + W_a^{AB} \quad (4)$$

where the superscripts D and AB denote dispersive and acid–base interactions, respectively.

Generally, the work of adhesion is coupled to ΔG_m^{ads} according to [29]:

$$\Delta G_m^{ads} = -N \cdot a \cdot W_a \quad (5)$$

where N is Avogadro's number and a is the surface area of a single probe molecule.

Fowkes has shown that the dispersive component of the work of adhesion can be estimated with the well-known geometric mean approach:

$$W_a^D = 2\sqrt{\gamma_L^D \cdot \gamma_S^D} \quad (6)$$

where γ_L^D and γ_S^D are the dispersive component of the the surface energy of the liquid (i.e. the probe) and the solid, respectively.

For the determination of the surface free energy with IGC normally *n*-alkane probes are employed. For these non-polar compounds it is safe to assume that interactions at the surface are purely of a dispersive nature.

In that case the combination of Eqs. (2) and (4) (with $W_a^{AB}=0$) and Eqs. (5) and (6) yields the following result [29]:

$$RT \cdot \ln(V_n) = 2N \cdot a \cdot \sqrt{\gamma_L^D \cdot \gamma_S^D} + C \quad (7)$$

By measuring the net retention volume for various alkane probes and, subsequently, plotting $RT\ln(V_n)$ as function of $a(\gamma_L^D)^{0.5}$, the disperse component of the surface free energy (i.e. surface tension) can be determined from the slope of a linear fit. Numerous IGC studies have shown that the linear relationship predicted by Eq. (7) agrees well with the experimental data [30].

Using the above mentioned methodology Schultz and coworkers have demonstrated that the γ_S^D values obtained with IGC correspond well with the results of the more traditional but also laborious and less accurate contact angle measurements [7]. However, authors have also stressed the difficulties associated with the determination of the molecular area, especially for non-spherical molecules such as straight chain alkanes [29]. The molecular area of the probes can be estimated from their liquid densities, assuming a spherical molecular shape in a hexagonal close-packed configuration [28]:

$$a = 1.09 \cdot 10^{14} \cdot \left(\frac{M}{\rho \cdot N} \right)^{2/3} \quad (8)$$

Another approach was adopted by Schultz and coworkers [7] who determined the molecular areas of alkanes from IGC isotherm measurements on reference solids. To circumvent the problems associated with the probe molecular area, Dorris and Gray [27] considered the adsorption characteristics of single methylene groups in the *n*-alkane probes. By defining the increment in free energy of adsorption per $-CH_2-$ unit, γ_S^D can be determined from:

$$\gamma_S^D = \frac{\left(RT \cdot \ln\frac{V_n(C_{n+1}H_{2n+4})}{V_n(C_nH_{2n+2})}\right)^2}{4(N \cdot a(CH_2))^2 \cdot \gamma(CH_2)} \quad (9)$$

The benefit of this approach lies in the fact that despite the use of various *n*-alkane probes (indicated by their structural formula C_nH_{2n+2}) only the methylene area, $a(CH_2)$, and surface tension, $\gamma(CH_2)$, have to be known. The CH_2 area is taken as 0.06 nm^2 based on a C–C bond length of 0.127 nm and an average distance of 0.47 nm for two CH_2 groups in adjacent molecules, which generally holds for *n*-alkanes in the bulk liquid [27]. Jacob and Berg [28] have found an excellent agreement between *n*-alkane molecular areas as determined from the fitting of experimental adsorption isotherms to the BET model and as obtained by simply assuming an area of 0.06 nm^2 for each methylene group. This indicates the validity of the approach. The parameter $\gamma(CH_2)$ is usually estimated from the surface tension of a linear polyethylene melt as function of temperature. Through extrapolation a value of 35.6 mJ/m^2 is obtained at 293 K, and $d\gamma(CH_2)/dT$ is taken as -0.058 $mJ/(m^2\ K)$. Similar values are also obtained when data from *n*-alkanes are extrapolated to infinite chain length [27].

In all the approaches described above, *a* is assumed to be independent of temperature, orientation of the probe, and interaction with the solid surface. These assumptions are by no means theoretically and experimentally sound [29]. Dorris and Gray stated that $a(CH_2)$ actually should be seen as an adjustable parameter [27].

Table 1
List of polar probes commonly used for characterization of acid–base interactions with IGC[a]

Probe	Character	AN* (kcal/mol)	DN (kcal/mol)
Water	amphoteric	15.1	18.0
Acetic acid	amphoteric	14.2	
Methanol	amphoteric	12.0	20
Ethanol	amphoteric	10.3	19
Formamide	amphoteric	9.3	24
n-Butanol	acidic (s)	9.1	
Chloroform	acidic (m)	5.4	0
Acetonitrile	amphoteric	4.7	14.1
Nitromethane	acidic (m)	4.3	2.7
Dichloromethane	acidic (m)	3.9	0
Dimethylsulfoxide	amphoteric	3.1	29.8
Acetone	amphoteric	2.5	17.0
Dichloroethane	acidic (w)	1.8	
Methylacetate	amphoteric	1.6	16.5
Ethylacetate	amphoteric	1.5	17.1
Diethylether	amphoteric	1.4	19.2
Carbon tetrachloride	apolar	0.7	0
Tetrahydrofuran	basic (m)	0.5	20.0
Benzene	apolar	0.17	0.1
Pyridine	basic (m)	0.14	33.1
Benzonitrile	basic (w)	0.06	11.9
Dioxane	basic (w)	0	14.8
t-Butylamine	basic (s)	0	57.5
Diethylamine	basic (s)	0	58.0
Triethylamine	basic (s)	0	61.0

[a] The corresponding donor and corrected [35] acceptor numbers were taken from [7,12,29,30,35,36]. w = weak, m = medium, s = strong.

2.2. Characterization of acid–base interactions at surfaces

After the dispersive interactions at a solid surface have been investigated with the use of *n*-alkane probes, acid–base interactions can be studied by injecting polar probes. For these probes, W_a^{AB} is usually not equal to zero, which leads to increased net retention volumes as compared to the *n*-alkanes. If an acidic probe exhibits a very high V_n value, this of course will be indicative of the basicity of the surface under investigation and vice versa. A list of polar probes which are commonly used in IGC is provided by Table 1.

To study (Lewis) acid–base (i.e., electron acceptor–electron donor) interactions in a more quantitative manner Eq. (7) can be employed [31]. If the molecular area and the dispersive component of the surface tension of the polar probe are known, the difference between V_n and the corresponding value on the *n*-alkane reference line (V_n^{ref}) is directly related to $\Delta G_m^{ads,AB}$:

$$\Delta G_m^{ads,AB} = -RT \cdot \ln\left(\frac{V_n}{V_n^{ref}}\right) \quad (10)$$

However, the determination of the appropriate *a* and γ_L^D values of polar probes is cumbersome due to the presence of one or more functional groups. To avoid these problems alternative methods have appeared in literature in which $\ln(V_n)$ is plotted as function of the logarithm of the saturated vapor

pressure [37] or the boiling point [38] of the probes. Such plots also exhibit similar straight line dependencies for *n*-alkanes and are much easier to construct as vapor pressure and boiling point data are readily available. A comparison of the three methods was provided by Panzer and Schreiber [30] who found almost identical $\Delta G_m^{ads,AB}$ for various probes on polycarbonate irrespective of the graphical representation. However, Donnet and coworkers [39,40] obtained useless results with the above stated methods when analyzing materials with relatively high dispersive components of the surface energy (>100 mJ/m^2) such as graphite powders and carbon fibers. For these materials lower V_n values were found for the polar probes compared to the reference alkanes. This problem was not encountered when $\ln(V_n)$ was plotted as function of the so-called molar deformation polarization, P_D, of the probe, defined as:

$$P_D \approx \frac{4}{3}\pi \cdot N \cdot \alpha = \frac{n_r^2 - 1}{n_r^2 + 2} \cdot \frac{M}{\rho} \quad (11)$$

where α is the polarisability and n_r is the refractive index of the probe.

The latter expression in Eq. (11) is obtained from the well-known Clausius–Mosotti equation realizing that n_r^2 equals the relative dielectric constant. Because probe density, mass, and refractive index data are easily retrieved from literature, P_D is also a factor which is readily accessible. In a later stage the approach was further improved by accounting not only for deformation but also for orientation polarizability. In this improved method so-called characteristic electronic frequencies of the probes are employed [40].

It should be noted that the use of T_b, $\log(P)$, or P_D will not enable a straight forward determination of γ_S^D. Recent theoretical developments have shown the direct relationship between $a(\gamma_S^D)^{0.5}$ and $\log(P)$ [37] and P_D [40]. However, the direct determination of the dispersive component of the surface energy from the latter two parameters requires the knowledge of awkward parameters. Therefore, for the determination of γ_S^D the method proposed by Dorris and Gray is preferred.

The final step in the characterization of acid–base phenomena on surfaces is the coupling of the thermodynamic data to empirical parameters which express (on a relative scale) the nature and magnitude of the interactions. These parameters can be regarded as acid and base indices of the material under investigation. To this end usually the enthalpy of the specific adsorption, $\Delta H_m^{ads,AB}$, is used [29]. This parameter can be determined by measuring $\Delta G_m^{ads,AB}$ as function of temperature and using the following relationship:

$$\Delta G_m^{ads,AB} = \Delta H_m^{ads,AB} - T\Delta S_m^{ads,AB} \quad (12)$$

where $\Delta S_m^{ads,AB}$ is the specific contribution to the change in entropy due to adsorption per mole of probe.

Thus the enthalpy factor can be obtained from the slope of a plot of $(\Delta G_m^{ads,AB}/T)$ as function of $(1/T)$ [30].

To obtain acid and base indices of surfaces, the probes have to be classified on the basis of acidity and basicity. Generally, the Drago and Gutmann approaches are used for this purpose. Both empirical procedures have strong and weak points as is discussed in the comprehensive review on acid–base interactions by Mukhopadhyay and Schreiber [29]. The Drago approach correlates the heats of acid–base complexation in organic liquids to four empirical parameters [29]:

$$-\Delta H = E_A \cdot E_B + C_A \cdot C_B \quad (13)$$

where subscripts A and B denote acid and base, respectively.

The *E* parameters correspond to the electrostatic contributions and the *C* parameters to the covalent contributions to the overall acid–base interaction. Although the Drago approach differentiates between so-called ''hard'' (electrostatic) and ''soft'' (covalent) interactions, its main drawback is the inability to describe amphoteric behaviour. Furthermore, the use of four probe parameters in a limited IGC data set often leads to overfitting phenomena and poor overall correlations.

Therefore, the Gutmann donor–acceptor concept is more frequently applied in IGC studies [29]. A probe is classified by only two empirical parameters, the donor number (DN) and the acceptor number (AN). These parameters describe the basic and acidic nature, respectively. The DN values (unit: kcal/mol) correspond to the enthalpy of formation for the

adduct produced when the base in question reacts with the reference Lewis acid $SbCl_5$ in the neutral solvent 1,2-dichloromethane (10^{-3} M). Unfortunately, no appropriate similar reference system was found for the characterizations of acids. Therefore, the AN value was measured as a relative induced shift in the ^{31}P NMR spectra of the base Et_3PO_4 when this compound was dissolved in the acid under investigation. A relative scale was introduced by setting the AN value to zero for the shift in *n*-hexane and setting the value to 100 for the shift for Et_3PO_4 in a dilute solution of the reference acid $SbCl_5$ in 1,2-dichloroethane. It should be noted that this approach is somewhat inconsistent as DN values are expressed in kcal/mol whereas AN is dimensionless. Furthermore, Riddle and Fowkes [35] showed that spectral shifts can also respond to dispersive interactions (i.e., v/d Waals forces) and that as a result non-zero AN values were obtained for various apolar probes. They corrected the reported AN values by subtracting the v/d Waals contribution. Furthermore, the corrected values were scaled to the enthalpy of the reaction of Et_3PO_4 with $SbCl_5$. By these two steps a new and consistent acceptor number, AN*, was defined having the same unit as the DN value. Both values are given for various probes in Table 1.

When for a set of probes, which covers the entire spectrum of possible interactions, the measured $\Delta H_m^{ads,AB}$ values are correlated to the acid and base indices of the probes it is possible to determine analogous parameters which indicate surface acidity–basicity. For this purpose usually the following correlation is used:

$$-\Delta H_m^{ads,AB} = K_a \cdot DN + K_b \cdot AN^* \quad (14)$$

where K_a and K_b are indices reflecting the acidity (electron acceptor) and basicity (electron donor) of the solid surface.

According to Eq. (14) a plot of $(-\Delta H_m^{ads,AB}/AN^*)$ versus (DN/AN*) should yield a straight line from which K_a can be obtained from the slope and K_b from the intercept. The indices provide an empirical basis for the classification of solid materials with respect to acidity–basicity [29]. It should be noted that Eq. (14) is exclusively of an empirical nature. Therefore, other relationships have been proposed in literature when the corresponding plots lacked satisfactory linearity [41].

It should be noted that very recently Goss [42] has proposed the use of surface free energy based acid–base parameters instead of the Gutmann approach. In this way no discrepancy is introduced as both dispersive and specific interactions are expressed as surface free energies. However, additional evaluation of this new method is still required [42].

For the IGC study of composites it has been attempted to correlate the acid–base parameters of the fiber surface and the matrix to the extent of adhesion. Schultz and coworkers [7] introduced a pair interaction parameter, *I*, describing the acid–base interaction between carbon fibers and an epoxy matrix according to:

$$I = K_a^f \cdot K_b^m + K_b^f \cdot K_a^{mf} \quad (15)$$

where the superscripts f and m denote fibre and matrix, respectively

It should be noted that also other pair interaction parameters have been defined with for instance also $K_a \times K_a$ and $K_b \times K_b$ terms to incorporate repulsive interactions at the interface [29]. The adhesion at the interface is usually evaluated from the shear resistance, τ. This shear resistance at the interface can be measured by means of mechanical fracturing techniques [43]. If a clear correlation between *I* and τ is found, acid–base interactions will have a strong influence on the interface adhesion. Such a correlation was obtained for untreated and modified carbon fibers in epoxy matrices [7]. A clear increase in shear resistance was obtained by applying a coating to the carbon fibers. In another study by Felix and coworkers [11] (who used a slightly different definition of the pair interaction parameter) also a straightforward correlation was found between stress related parameters and the pair interaction parameter for various modified cellulose fibers in a polystyrene matrix. A plasma treatment of the fibers in the presence of methacrylic acid vapor clearly increased fibre–matrix adhesion. However, for the same fibers in a chlorinated polyethylene matrix no clear correlation was observed.

2.3. Heterogeneity of adsorption site energy

Interactions of probes with fiber surfaces are usually studied at infinite dilution to prevent probe–

probe interactions. However, working at these low probe loadings can also have consequences for the probe–surface interactions when the surface has an interaction energy distribution. Decreasing the amount of injected probe will then lead to a preferential sampling of the high energy sites and thus to enhanced interaction. In the literature very little can be found on concentration effects in the IGC characterization of fibers. Very recently the distrtibution function of the adsorption site energies of treated and untreated carbon fibers with IGC has been evaluated [44]. Also in this work it will be shown how the study of probe–surface interaction as function of probe concentration can yield valuable information on surface energy heterogeneity of fibers. The study of surface site heterogeneity has been more common for the IGC characterization of active solids such as fillers [45], pigments [46], silicas [47,48], and clays [49].

When at any given probe concentration symmetrical, flow independent elution profiles are obtained, fluctuations in the surface free energy can directly be determined with the methodology outlined above while varying the amount of probe [46]. However, in most cases an adsorption isotherm at infinite dilution has to be measured to correctly correlate probe concentration effects in IGC to the energetic heterogeneity of the surface. From the mass balance equation of the IGC column the following relationship can be derived [50]:

$$q_i = \frac{1}{mRT}\int_0^{p_i} V_n \cdot dp_i \qquad (16)$$

where $q_i$is the amount of adsorbed probe divided by the mass of stationary phase, m, in the IGC column, and p_i is the partial pressure of the probe.

The partial pressure at a given time point can be obtained from the detector signal. The corresponding adsorbed amount can be found from a specific area from a chromatogram which is determined by Eq. (16) and the shape of the elution profiles [51]. Generally isotherms at infinite dilution are constructed with either the peak maxima (PM) or the elution by characteristic point (ECP) method. With the PM method varying amounts of probe are injected onto the IGC column. Through the observed peak maxima a smoothed curve is drawn and the isotherm is determined from this curve. When the diffusive peak flanks of the elution profiles at various probe concentrations overlap the less laborious ECP method can be employed. The adsorption isotherm is then constructed from the diffusive peak flank of the elution profile of a single injection of a relatively large amount of probe.

The overall, measured, adsorption isotherm, $\theta_t(p,T)$, is for a heterogeneous surface energy related to the local isotherm, $\theta_l(\epsilon,p,T)$, via the adsorption energy distribution function, $F(\epsilon)$,

$$\theta_t(p,T) = \int_{\epsilon_{min}}^{\epsilon_{max}} \theta_{lt}(\epsilon,p,T) \cdot F(\epsilon) \cdot d\epsilon \qquad (17)$$

where ϵ_{max} and ϵ_{min} indicate the range in potential energy of adsorption.

For the determination of $F(\epsilon)$ (which is an indicator of site energy fluctuations) from Eq. (17) an assumption on the shape of the local isotherms has to be made and usually complex numerical analysis is required [45,47–49].

3. Experimental

3.1. Fibers

The fiber materials given in Table 2 have been characterized in this work.

3.2. Probes

All chemicals were of analytical-reagent grade (purity of at least 99%). Butane miconox cylinders were obtained from Chrompack (Middelburg, The Netherlands). Pentane, heptane, octane, dichloromethane (DCM), diethyl ether, chloroform, toluene, and tetrahydrofuran (THF) were obtained from Fluka (Zwijndrecht, The Netherlands). Acetone, acetonitrile (ACN), hexane, and benzene were purchased from Baker (Deventer, The Netherlands). For all IGC studies methane was used to determine the dead volume. To ensure low injection amounts only probe

Table 2
Fiber samples studied in this work[a]

Trade name	Manufacturer	Lot no. or prod. date	Surface treatment	Specific area (m^2/g)	Sample code
HTA 5000	Tenax	61011	–	0.37	TEN1
HTA 5001	Tenax	60312	thermal	0.37	TEN2
HTS-12k/5000	Tenax	70892	–		TEN3
HTS-12k/5001	Tenax	70892	electrochemical		TEN4
Twaron	Akzo Nobel	2-18-1997	–	0.22	TWA1
Twaron	Akzo Nobel	2-18-1997	standard sizing	0.22	TWA2
Twaron	Akzo Nobel	2-18-1997	epoxy sizing	0.22	TWA3

[a] The sample code is used in the text to indicate the fiber material.

vapor was injected by adding a few drops of the liquid probe to an autosampler vial, capping the vial, and injecting the gas in the vial. To study concentration effects, gas injections were made repetitively from the same vial. In between injections the syringe was flushed 15 times with gas from the vial to decrease the probe concentration in the gas phase.

3.3. Preparation of IGC fiber columns

Fiber columns were prepared by pulling intact fiber bundles through home made glass columns with a length of 30 cm and an internal diameter of 1.9 mm. The excess fiber material at both column ends was cut, resulting in columns loaded with approximately 0.7 g of Tenax carbon fibers or 0.5 g of Twaron fibers. With this procedure tightly packed glass IGC columns are produced that can contain up to 40 000 individual fiber threads. As the fibers are not chopped [25], no additional surface is created during IGC column preparation.

3.4. IGC measurements

The IGC analyses of the fibers were performed on a modified Fisons Model 8530 Mega 2 gas chromatograph equipped with a constant flow regulator, an EL 980 electrometer for flame ionization detection, and an AS 800 autosampler (Interscience, Breda, The Netherlands). A gas tight SGE GT series II syringe (Alltech, Breda, The Netherlands) was installed in the autosampler to inject 1–5 μl of gaseous probe. In the split outlet an ENMF 0–250 mbar pressure sensor and a Porter 9000-AMVF-15 back pressure regulator (Interscience, Breda, The Netherlands) were installed to ensure a stable low head pressure in the range of 25–55 mbar (corresponding to a N_2 carrier flow-rate of 1–1.5 ml/min through the fiber columns) in combination with a high split flow of 50–100 ml/min. A Fisons cryo unit 820 (Interscience, Breda, The Netherlands) controlling a magnetic valve coupled to the GC and a liquid nitrogen dewar enabled the measurement at subambient temperatures. Probe retention on the fiber columns was measured isothermally in the range of 0–100°C. The fiber columns were connected to injector and detector via deactivated fused-silica capillaries with an internal diameter of 0.53 μm (Interscience, Breda, The Netherlands) which were connected to the column via 1/8″–1/16″ Swagelock couplings (type B-200-6-1; Alltech, Breda, The Netherlands) with teflon ferrules. Prior to analysis the columns of bare fiber materials were conditioned at 150°C for 16 h and IGC columns with sized fibers were treated for the same period at 110°C. A schematic representation of the IGC set-up is depicted in Fig. 1.

4. Results and discussion

4.1. Measurement of γ_S^D values of fiber surfaces

In this work three methods for the determination of γ_S^D values from the measured net retention volumes of *n*-alkane probes have been evaluated. In Table 3 the γ_S^D values are listed of two Tenax carbon fibers (with and without thermal treatment) and three Twaron fibers (a material as such and two sized batches). As was demonstrated by Schultz and

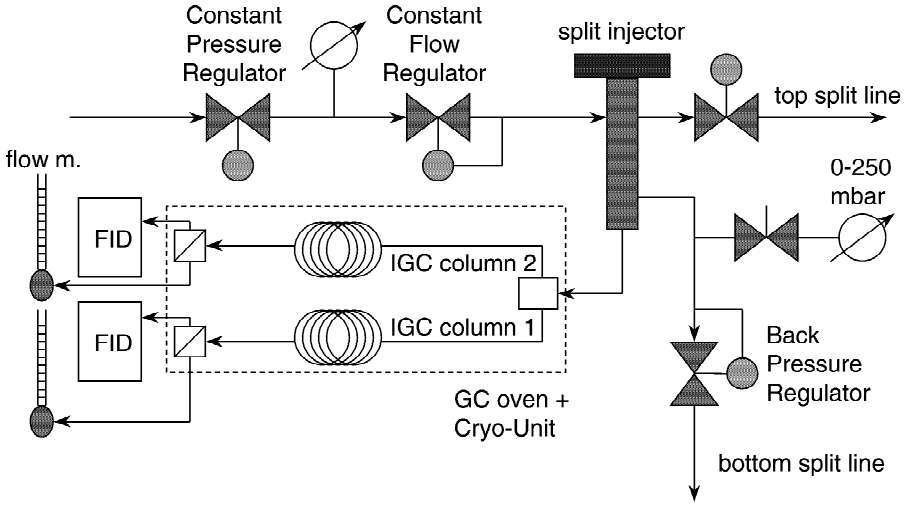

Fig. 1. Schematic representation of IGC set-up.

coworkers [7] for various carbon fibers, we also found a good agreement between the γ_S^D values determined with methods 2 and 3. Indeed, Jacob and Berg [28] found that the molecular area of *n*-alkanes on CTMP fibers as determined with the Dorris–Gray method (with 0.06 nm^2 per CH_2 group) agreed very well with the *a* values obtained from BET isotherm measurements. Furthermore, our data clearly show that the molecular area can not be estimated correctly with the use of Eq. (8). This leads to unrealistically high γ_S^D values. In our IGC screening studies (see Section 4.5) we employ the Dorris–Gray method because the calculations are easily automated with a spread sheet program.

Table 3
Determination of the dispersive component of the surface energy of Tenax carbon and Twaron fibers according to different methods[a]

Fiber	T (°C)	γ_S^D (mJ/m^2)		
		Method 1	Method 2	Method 3
TEN1	79	217	89	93
TEN2	79	204	81	87
TWA1	39	109	50	44
TWA2	39	72	31	29
TWA3	39	96	38	38

[a] Method 1: calculated according to Eq. (8); method 2: with measured *a* values [7]; method 3: on the basis of $a(CH_2)$ and $\gamma_S^D(CH_2)$ [27].

As to our knowledge no IGC studies on Twaron fibers have been reported in the literature, the corresponding γ_S^D values given in Table 2 cannot be compared with published data. However, data on the dispersive interactions at Tenax HTA 5000 carbon fiber surfaces have been reported. Jacobasch and coworkers [24] found a γ_S^D value of 84 mJ/m^2. Unfortunately, they do not state the specific temperature for this measurement. The same group also reports a value of 79 mJ/m^2 for the same material at 40°C [16]. Although these data seem to be comparable to our results, the temperature dependence of γ_S^D has to be considered. In Figs. 2 and 3 the temperature dependence is depicted for the Tenax carbon and Twaron fibers, respectively. These figures show that with the exception of the untreated Twaron material the γ_S^D values decrease linearly with temperature. The decrease of γ_S^D with T is generally attributed to the entropic contribution to the surface free energy [18,19]. A linear decrease over a limited temperature range has also been described in the literature for several fiber samples [19,20]. Possibly, the non-linear temperature dependence could indicate additional temperature dependent processes which modify the surface. Thermal conditioning of the IGC column can be very important in this respect. However, the TWA1 IGC column was conditioned for 16 h at 150°C.

For both Tenax carbon fibers the γ_S^D values

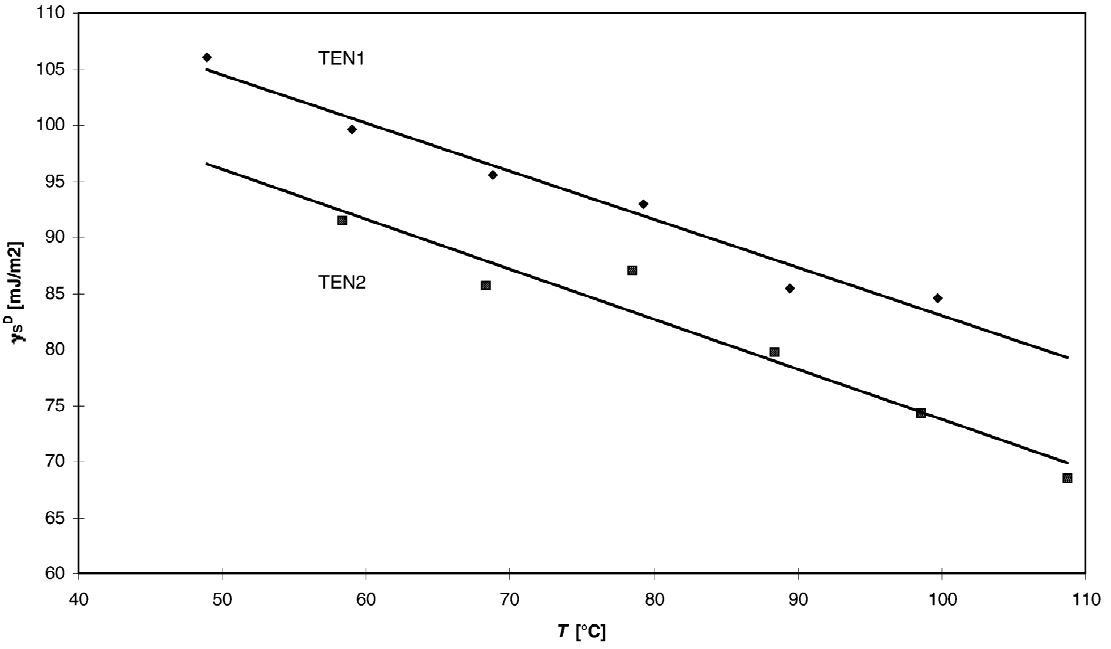

Fig. 2. Temperature dependence of γ_S^D for TEN1 and TEN2 [trend line TEN1: γ_S^D (mJ/m^2) $= -0.429 \times T$(°C) $+ 125.91$] [trend line TEN2: γ_S^D (mJ/m^2) $= -0.444 \times T$(°C) $+ 118.22$].

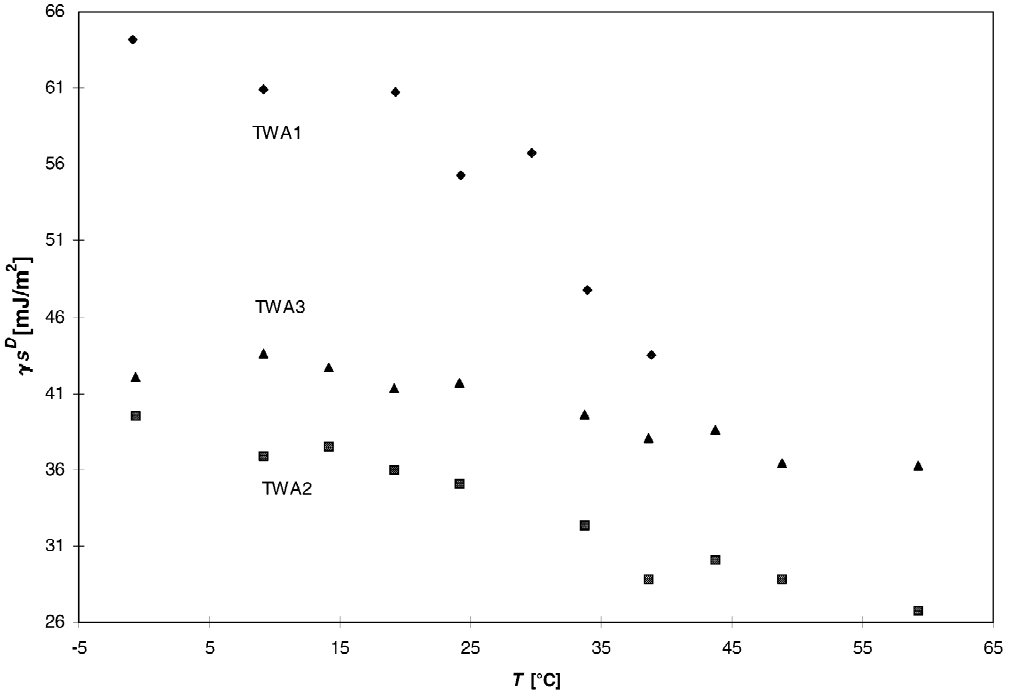

Fig. 3. Temperature dependence of γ_S^D for TWA1, TWA2, and TWA3.

decrease with 0.45 mJ/°C m^2 whereas for the sized Twaron fibers a decrease of approximately 0.2 mJ/°C m^2 was observed. Through extrapolation values of 21 and of 30 mJ/m^2 are obtained at 80°C for the TWA1 and TWA2 fiber, respectively. As expected γ_S^D is much higher for the active carbon fiber than for the sized Twaron material. In the same manner a γ_S^D value of approximately 108 mJ/m^2 is estimated for the Tenax carbon fibers at a temperature of 40°C. Unfortunately, this temperature corrected value does not agree well with the data of Simon et al. [16].

Finally, it should be noted that the temperature range over which γ_S^D can be determined accurately is limited experimentally. At too high temperatures the net retention volume of the *n*-alkanes becomes almost zero while at very low temperatures retention becomes so strong that analysis times and peak broadening become excessive. The optimal temperature range is of course dependent on the *n*-alkane probes that are employed (higher *n*-alkanes are less volatile) and the fiber surface itself. For active surfaces as for instance observed for carbon fibers IGC measurements are usually conducted at relatively high temperatures.

4.2. Determination of consistent ΔG_m^{ab} values of probe–fiber interactions

Contrary to the work of Panz and Schreiber, who studied polycarbonate surfaces with IGC [30], our results indicate that $\Delta G_m^{ads,AB}$ values for probe–fiber surface interactions do depend on the data treatment in IGC. Just as Donnet and coworkers [39,40] we also measured negative $\Delta G_m^{ads,AB}$ values for the interaction of almost all polar probes with Tenax carbon fibers when $RT\ \ln(V_n)$ is plotted as function of $a(\gamma_S^D)^{0.5}$, T_b, or $\log(P)$. For carbon fibers which possesses a relatively high dispersive component of the surface free energy, consistent and reproducible acid–base interaction energy data were only obtained when the P_D method was employed. However, as Figs. 4–7 indicate, the various methods to determine acid–base interactions also lead to different $\Delta G_m^{ads,AB}$ values for the IGC characterization of energetically more moderate fibers such as Twaron.

These results indicate that for polar probes on fiber surfaces it is very difficult to accurately determine the dispersive component of the interaction energy. Although it does not prove that the P_D method yields

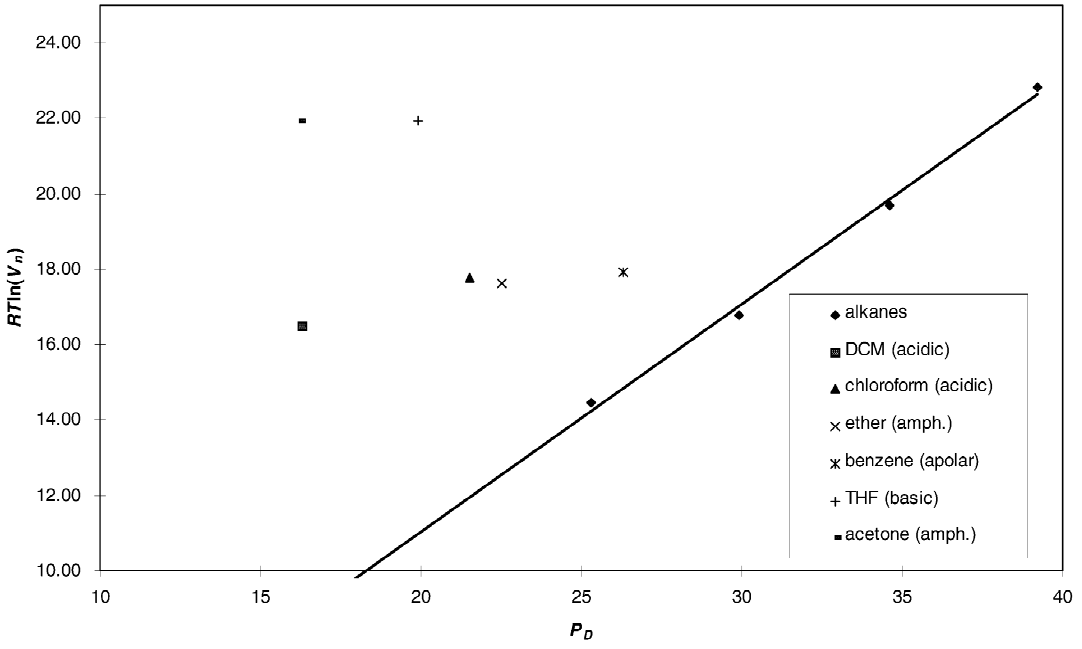

Fig. 4. Determination of $\Delta G_m^{ads,AB}$ for polar probes on TWA1 at 38.8°C with the P_D method [alkane trend line: $RT\ln(V_n) = 0.603 \times P_D$ (cm^3/mol) − 1.025).

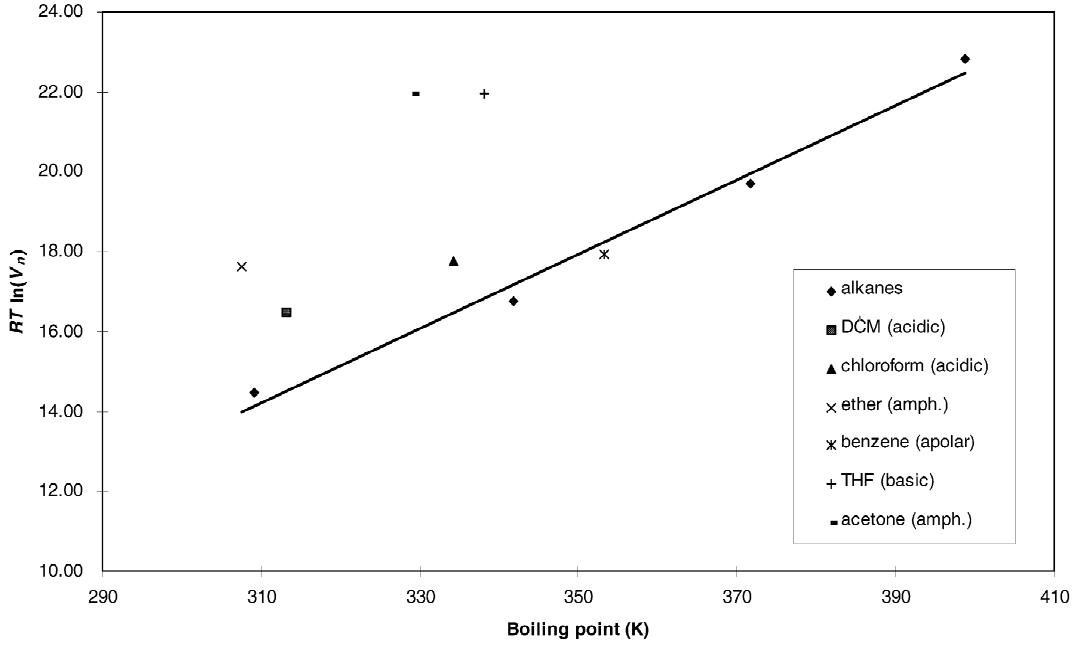

Fig. 5. Determination of $\Delta G_m^{ads,AB}$ for polar probes on TWA1 at 38.8°C with the T_b method [alkane trend line: $RT\ln(V_n) = 0.093 \times T_b(K) - 14.73$].

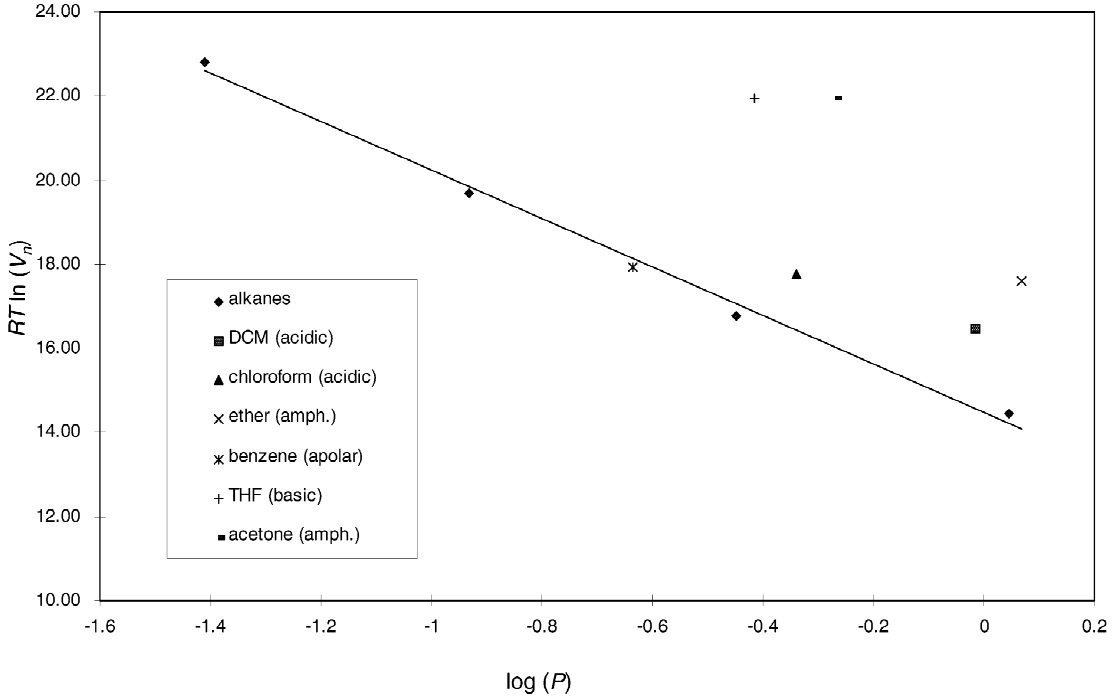

Fig. 6. Determination of $\Delta G_m^{ads,AB}$ for polar probes on TWA1 at 38.8°C with the log(P) method [alkane trend line: $RT\ln(V_n) = -5.772 \times \log(P) + 14.48$].

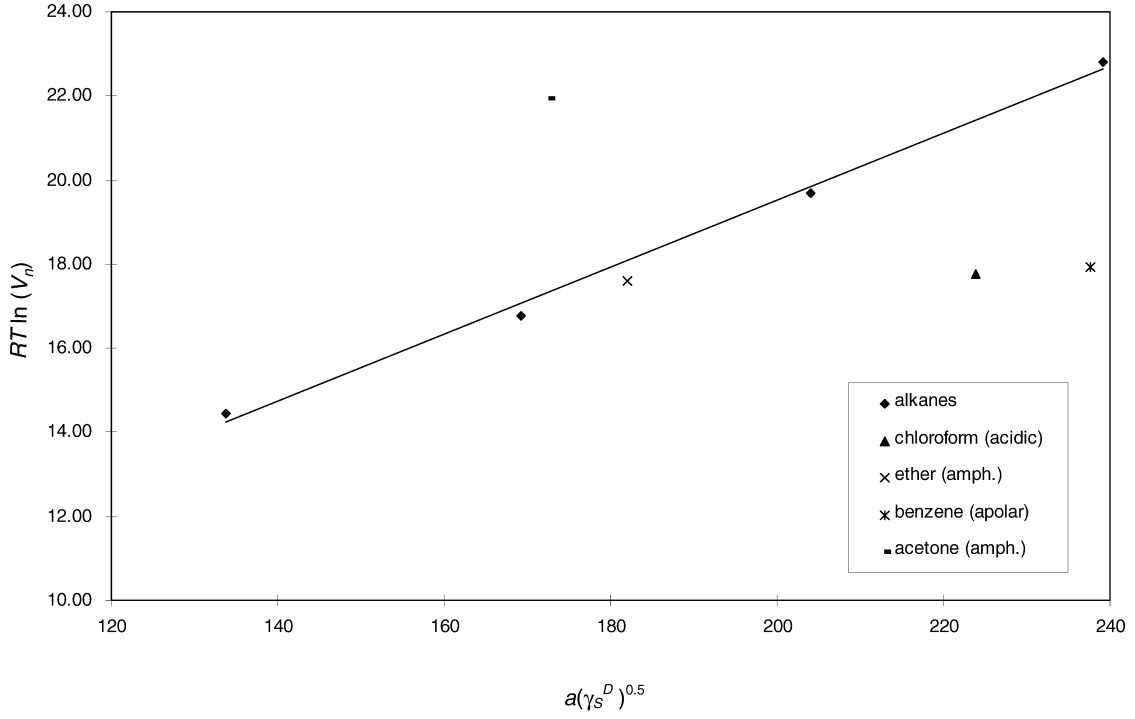

Fig. 7. Determination of $\Delta G_m^{ads,AB}$ for polar probes on TWA1 at 38.8°C with the $a(\gamma_S^D)^{0.5}$ method [alkane trend line: $RT\ln(V_n) = 0.0798 \times a(\gamma_S^D)^{0.5}$ (mJ$^{0.5}$ m) + 3.543].

the best estimate for this dispersive component, Fig. 4 clearly illustrates that with this method the dispersive interaction of the polar probes is relatively small compared to that of the *n*-alkanes (i.e., the data points for the polar probes are situated more to the left-hand side of the *n*-alkane reference line than with the other methods). Consequently, consistent $\Delta G_m^{ads,AB}$ data are obtained while also relatively high specific Gibbs energy values are measured for a reasonably apolar probe as benzene. However, when one uses IGC for the monitoring of the surface characteristics of a fiber material in a production plant it is not absolutely necessary to determine the dispersive component of polar probes correctly. By comparison of the $\Delta G_m^{ads,AB}$ values of various probes from batch to batch it is possible to detect fluctuations in surface characteristsics of the fibers (see Section 4.5).

Because of the discussion given above and the fact that the P_D value of the probes is so easily obtained, we selected the P_D method to determine the acid–base interaction energy of the polar probes on fiber surfaces. It should be noted that recently also consistent and reproducible results are reported with the use of the linear free energy relationships [52]. However, we have not evaluated this IGC data treatment procedure because of all the probes used in this work not all necessary parameters were available at the time.

4.3. Enthalpy measurements and the usefulness of K_a and K_b parameters

From the measurement of $\Delta G_m^{ads,AB}$ as a function of temperature the specific enthalpy in the corresponding temperature range can be obtained as is outlined in Section 2.2. For a number of probe–fiber combinations we have measured $\Delta H_m^{ads,AB}$ values according to the P_D, $a(\gamma_S^D)^{0.5}$, T_b, and log(*P*) method. Again most consistent results were obtained with the P_D method, with the other methods frequently non-linearity of the data was observed when $\Delta G_m^{ads,AB}/T$ was plotted as function of $1/T$. An

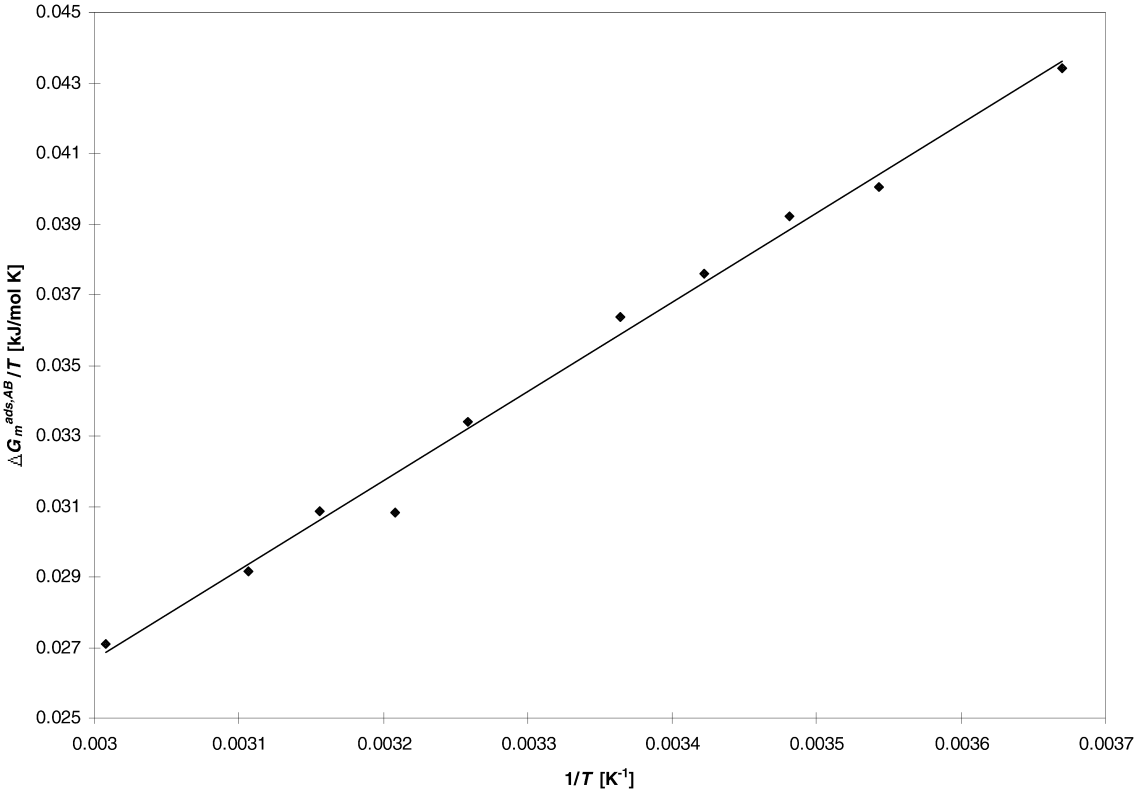

Fig. 8. Plot of $\Delta G_m^{ads,AB}/T$ as function of $1/T$ for DCM on TWA2 (with use of the P_D method) [trend line: $\Delta G_m^{ads,AB}/T$ (kJ/mol K) = 25.28/T (1/K) − 0.049).

example of such a plot with the P_D method is given in Fig. 8. An overview of the enthalpy data is provided in Tables 4 and 5. Due to the curve fitting procedure the relative standard deviation in the enthalpy data was approximately 10%, while for the $\Delta G_m^{ads,AB}$ data at a given temperature the relative standard deviation is roughly 2%. Note that the trends in the enthalpy data are clearly similar to the trends in the listed $\Delta G_m^{ads,AB}$ values (see also Section 4.5).

Table 4
Gibb's energy and enthalpy of acid–base interactions of polar probes on carbon fibers[a]

Probe	TEN1 (kJ/mol)		TEN2 (kJ/mol)	
	$\Delta G_m^{ads,AB}$	$\Delta H_m^{ads,AB}$	$\Delta G_m^{ads,AB}$	$\Delta H_m^{ads,AB}$
Dichloromethane	5.2	11.8	9.5	19.4
Chloroform	4.2	11.5	–	–
Ether	2.0	35.5	9.8	27.1
Acetonitrile	–	–	22.4	43.9
Acetone	6.8	14.3	20.4	47.1
Tetrahydrofuran	6.4	17.7	–	–
Benzene	3.2	4.4	–	–

[a] P_D method, $\Delta G_m^{ads,AB}$ values measured at 79°C, $\Delta H_m^{ads,AB}$ measured in the range of 58–109°C.

Table 5
Gibb's energy and enthalpy of acid–base interactions of polar probes on Twaron fibers[a]

Probe	TWA1 (kJ/mol)		TWA2 (kJ/mol)		TWA3 (kJ/mol)	
	$\Delta G_m^{ads,AB}$	$\Delta H_m^{ads,AB}$	$\Delta G_m^{ads,AB}$	$\Delta H_m^{ads,AB}$	$\Delta G_m^{ads,AB}$	$\Delta H_m^{ads,AB}$
Dichloromethane	7.7	39.2	9.6	25.3	8.6	17.7
Chloroform	5.8	28.3	9.4	23.3	8.2	15.7
Ether	5.1	6.0	2.5	3.6	2.0	–
Acetone	13.2	51.7	7.8	18.7	6.8	12.2
Tetrahydrofuran	11.0	46.6	7.8	16.1	7.1	11.0
Benzene	3.1	14.0	5.9	12.1	4.9	6.8

[a] P_D method, $\Delta G_m^{ads,AB}$ values measured at 39°C, $\Delta H_m^{ads,AB}$ measured in the range of 0–60°C.

When enthalpy data are available and the donor and acceptor numbers of the polar probes are known, the empirical relationship given by Eq. (14) can be used to establish the acid–base parameters of the fiber surface. Unfortunately, our data did not correlate well with Eq. (14). Only for the TWA1 fiber a linear correlation was found but solely when the T_b method was applied. From the plot given in Fig. 9 a K_a value of 1.1 and a K_b value of 2.0 were found, indicating an amphoteric–basic surface. However, this is not fully in agreement with the interaction energy data provided in Table 5 and knowledge on the chemical composition of Twaron. Rather than proposing other empirical relationships to correlate acid–base surface parameters, it is better to critically examine the additional value of the laborious measurement of these parameters. Of course the determination of K_a and K_b values enables a quantita-

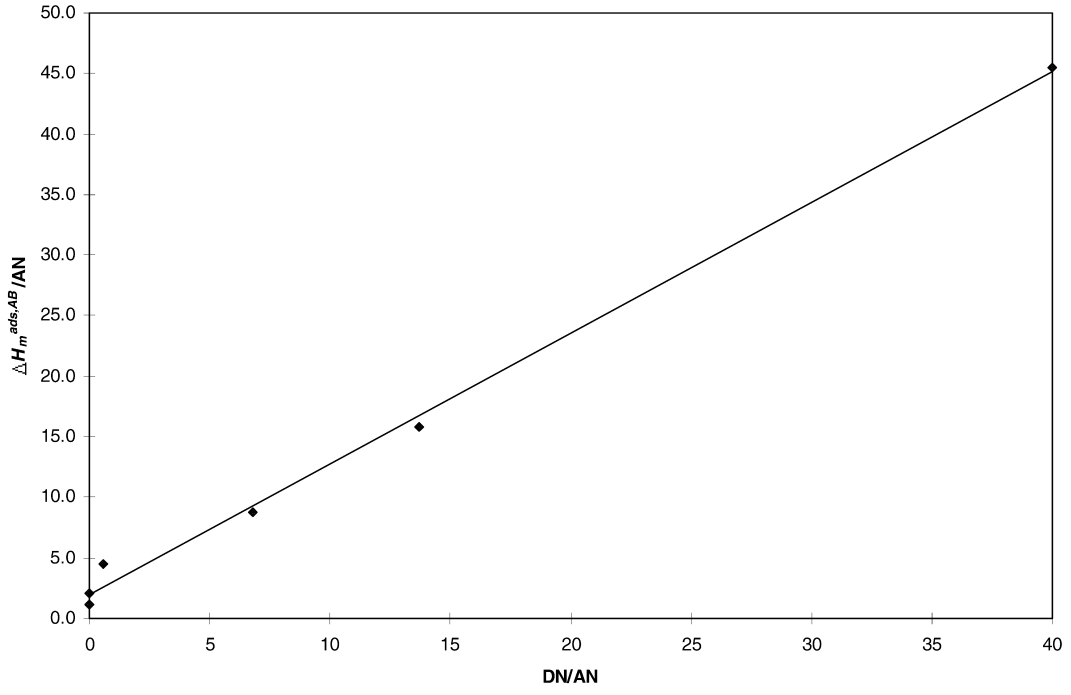

Fig. 9. Plot of $\Delta H_m^{ads,AB}$/AN as function of AN/DN TWA1 (with use of the T_b method) [trend line: $\Delta H_m^{ads,AB}$/AN = 1.077 × AN/DN + 2.007).

tive basis to correlate the acid–base character of the surface to composite strength [52]. However, when the data points are somewhat scattered around the linear regression curve as is the case in Fig. 9 the relative error in the K_a and K_b parameters rapidly becomes quite substantial. Especially the K_b value which is determined from the intercept of the linear regression line with the *y*-axis can only be measured with limited accuracy. With these substantial errors it will be often quite difficult to statistically prove that K_a is larger or smaller than K_b! When straightforward linear regression is used, the parameters are also highly dependent on the interaction energy data of THF because this probe exhibits such a substantial DN/AN value. Furthermore, data for purely acidic or basic probes are difficult to incorporate in such plots because DN/AN values are, respectively, zero or infinitely large.

For reasons listed above we developed a measurement scheme in which acid–base interactions are only studied by measuring Gibb's interaction energy values. This IGC procedure was devised to monitor the batch-to-batch surface characteristics of fiber materials (see Section 4.5). Because no enthalpy data and K_a and K_b parameters were determined, a single IGC characterization of a fiber batch could be performed in a couple of hours. Of course the discussion on the chemical nature of the fiber surface can with such a scheme only be of a qualitative nature.

4.4. Concentration effects in relation to energy heterogeneity of active sites

Generally, it is stated in the literature that probe concentrations should be very low in the IGC characterization of surface to prevent probe–probe interactions. Therefore, usually a small amount of gaseous probe is injected to ensure that the interactions are measured at infinite dilution of the probe. However, even at these low probe loadings concentration effects can exist, especially for materials with energetically more active surfaces such as carbon fibers. In Fig. 10 the overlay of ether elution profiles on a TEN2 fiber is shown. Above a given amount of injected probe the retention volume is almost independent of the probe concentration while below this amount the interaction of the probe with

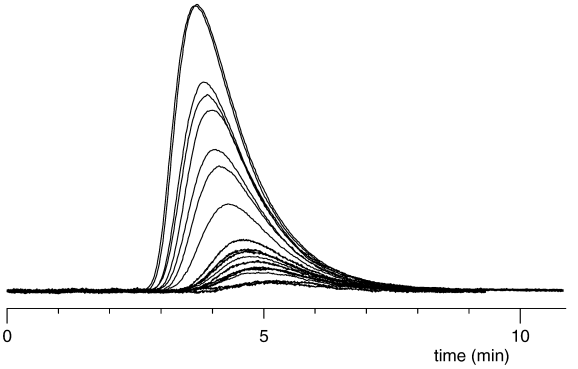

Fig. 10. Overlay of elution profiles of ether, injected in various amounts on TEN2 at 80°C.

the fiber surface suddenly increases (i.e., the retention volume increases). This type of concentration dependence at very low probe loadings was observed for acidic and basic probes on carbon fibers. A slight concentration dependence was also noticed for the bare Twaron fibers but in general for the aramid fibers studied in this work concentration effects were negligible.

It was established that this phenomenon was not caused by mass transport limitations as the net retention volume was not dependent on the flow-rate. The increased interaction at low probe concentration is indicative of the heterogeneity of the interaction energy of the active sites at the fiber surface. As less probe molecules are available, the favourable interaction with a limited number of active sites of high interaction energy affects the retention volume significantly. When the amount of injected probe is increased, the majority of probe molecules will interact with the more abundant sites of moderate interaction energy. Therefore, extrapolation of V_n to zero probe dilution will indicate the interaction with a few active sites of high interaction energy, while at higher probe concentration the net retention volume reflects the average interaction. As is discussed in Section 4.5, this concentration effect can vary significantly from batch to batch and is, therefore, an important surface characteristic for carbon fibers.

As Fig. 10 shows no overlapping peak flanks, we used the peak maxima (PM) method (see Section 2.3) to determine the adsorption isotherm at low probe concentration. After calibration with ether gas standards, the detector signal could be related to the

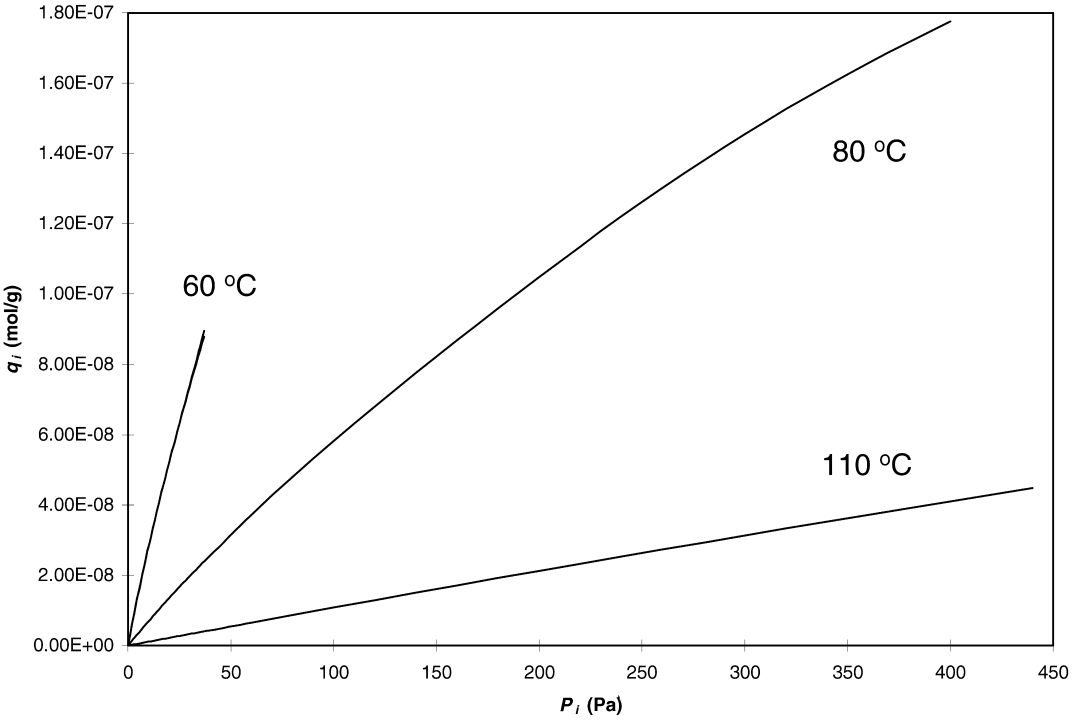

Fig. 11. Adsorption isotherms of ether on TEN2 at three different temperatures.

partial pressure of the probe. The time axis of Fig. 10 could easily be transformed to a V_n axis, with the use of the dead time and the flow-rate. It was found that a fourth degree polynomial fit of the PM data provided a good description of the net retention volume as a function of the vapour pressure. As a polynomial function is easily integrated, the adsorption isotherm construction according to Eq. (16) was straight forward. Fig. 11 shows the adsorption isotherms of ether on TEN2 for three different temperatures. The isotherms have a typical shape, at very low vapour pressures they resemble Langmuir isotherms, but at higher probe levels they do not flatten out but become linear (in this part of the isotherm the interaction is no longer affected by the probe concentration). The isotherms become more linear with increasing temperature indicating that the interaction with the sites of moderate interaction energy becomes more predominant at higher temperatures.

Several authors [45,47–49] have described mathematical methods to determine the interaction energy distribution function from the adsorption isotherm. However, due to the complex modelling required we did not calculate the energy distribution function from the presented isotherms.

4.5. IGC as a screening tool of the quality of industrial fibers

In our laboratory IGC is used routinely as a surface characterization tool for industrial fibers. In this paragraph two examples will be given which illustrate the possibilities and limitations of the technique in fiber characterization.

First of all, we employ the technique frequently to study Tenax carbon fibers. Carbon fibers are produced from the carbonization of PAN fibers. The production of carbon fibers is a very complex process and involves several high temperature treatments. The characteristics of the final material are dependent on many production parameters and the quality of the starting material. Furthermore, to promote adhesion in composites the surface of carbon fibers are usually activated thermally and/or

electrochemically and often also a fiber finish is applied. As carbon fibers are being used in composite materials for aeroplane construction, almost no variation in surface characteristics can be tolerated. In our laboratory, Tenax carbon fibers are studied with XPS and IGC. With XPS the elemental composition (and the oxidation state of elements) can be probed of the fiber surfaces. Combination of XPS data with IGC results often reveals the nature, cause and consequence of surface contaminations and irregularities. For the IGC analysis of batches of carbon fibers we have developed a straight forward procedure with which all relevant IGC information (i.e., dispersive and acid–base interaction and active site heterogeneity) is obtained within several hours. Examples of the data charts generated with this procedure are given given in Figs. 12 and 13. These charts correspond to a carbon fiber batch, respectively, before and after electrochemical surface treatment. Clearly, for this batch the electrochemical treatment has had a huge impact on the surface characteristics. The dispersive interactions have increased considerably. Both the acidic and the basic probes exhibit stronger interactions although the effect seems to be somewhat stronger for the basic probes. Note that solely on the basis of Gibbs energy data, it is difficult to classify a fiber as acidic or basic because the degree of acidity–basicity of the probes (i.e., the donor and acceptor numbers) is not considered. However, when various batches of the same fiber or the effect of a given surface treatment are under investigation such an absolute reference is not necessary. In that case the IGC data of the various materials can directly be compared. After the treatment a strong concentration effect was observed which was clearly most profound for the basic ether probe. This indicates that a number of very active acidic sites are formed due to the surface treatment.

Generally, no concentration dependent retention volume is observed for *n*-alkanes. In the chart the concentration effect of heptane is nonetheless included because we have found that a strong concentration effect of this probe is usually a very good indicator for irregularities in the column packing (e.g., dead volume due to insufficient fiber threads or preferential flow paths due to too many fiber threads).

The IGC technique was recently also applied in a study of Twaron fiber finishes. Twaron is a low-weight aramid fiber of exceptional strength. The material is applied in a variety of products such as composites, rubber tires, bullet proof vests and helmets. To give a Twaron-composite material enhanced durability a good adhesion of the fiber to the matrix is essential. To this end several fiber finishes are used. In this project the removal of fiber finish through Soxhlett extraction was studied. A Twaron fiber material as such, Twaron treated with a standard finish and Twaron with a new epoxide based finish were characterized with IGC before and after a 4-h Soxhlett extraction in ethanol. The results are given in Table 6. As expected Twaron as such is hardly affected by the extraction. In general, the interaction energy is slightly increased. A possible

Table 6
Dispersive component of the surface energy and the Gibb's energy of acid–base interactions of polar probes on Twaron fibers[a]

	TWA1		TWA2		TWA3	
	AS	ASE	AS	ASE	AS	ASE
γ_S^D (mJ/m^2)	52.9	51.8	36.3	48.8	40.0	32.3
$\Delta G_m^{ads,AB}$ (kJ/mol)						
Dichloromethane	8.3	8.3	10.9	8.3	9.0	6.8
Chloroform	6.5	6.1	10.3	6.0	8.4	6.0
Acetone	12.4	13.8	9.0	13.1	7.1	7.1
Acetonitrile	13.2	14.2	15.0	13.6	12.4	10.7
Dioxane	11.2	12.5	11.1	11.9	9.3	7.5
Ether	4.9	5.6	3.0	5.3	2.2	2.6
Tetrahydrofuran	10.7	11.9	9.0	11.1	7.6	6.3

[a] P_D method, γ_S^D and $\Delta G_m^{ads,AB}$ values measured at 40°C), with: AS = as such, ASE = after Soxhlett extraction.

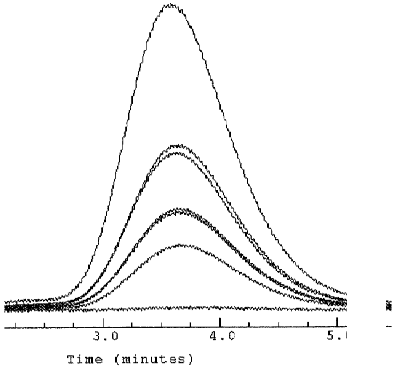

n-C7
flow: 1,28 ml/min

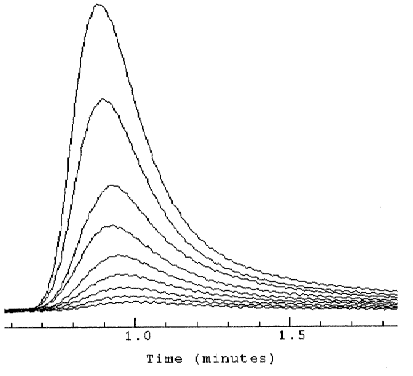

DCM
flow: 1,28 ml/min
dG(DCM): 7,9 - 9,5 kJ/mol

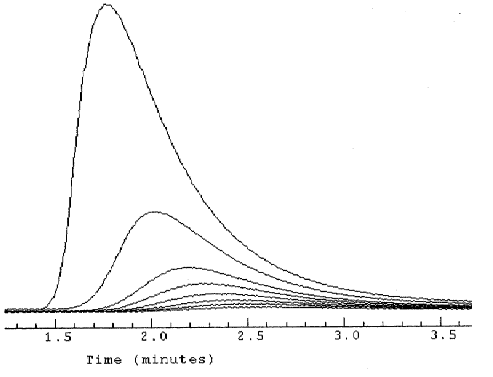

Di-ethylether
flow: 1,28 ml/min
dG(Ether): 7,9 - 9,6 kJ/mol

	Column	K0
	filaments	720
	pressure(mbar)	70
	flow(ml/min)	1.2
	temperature °C	80
mJ/m²	Y(d/s)	106.
dG (kJ/mol)	DCM	8.5
	Ether	8.1
	Acetonitrile	21.5
	Acetone	16.4
	Benzene	4.4
	Chloroform	5.2
	THF	13.5
	Dioxane	-

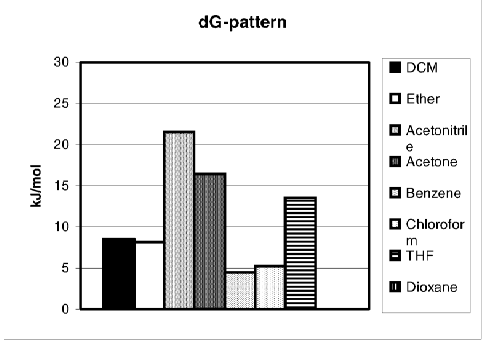

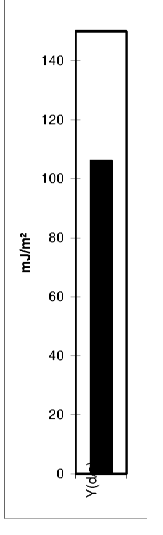

Fig. 12. IGC data chart of Carbon fiber TEN3 (without surface treatment; the Doris–Gray method is used to determine γ_S^D, and the P_D method is used to determine $\Delta G_m^{ads,AB}$, IGC measurements conducted at 80°C).

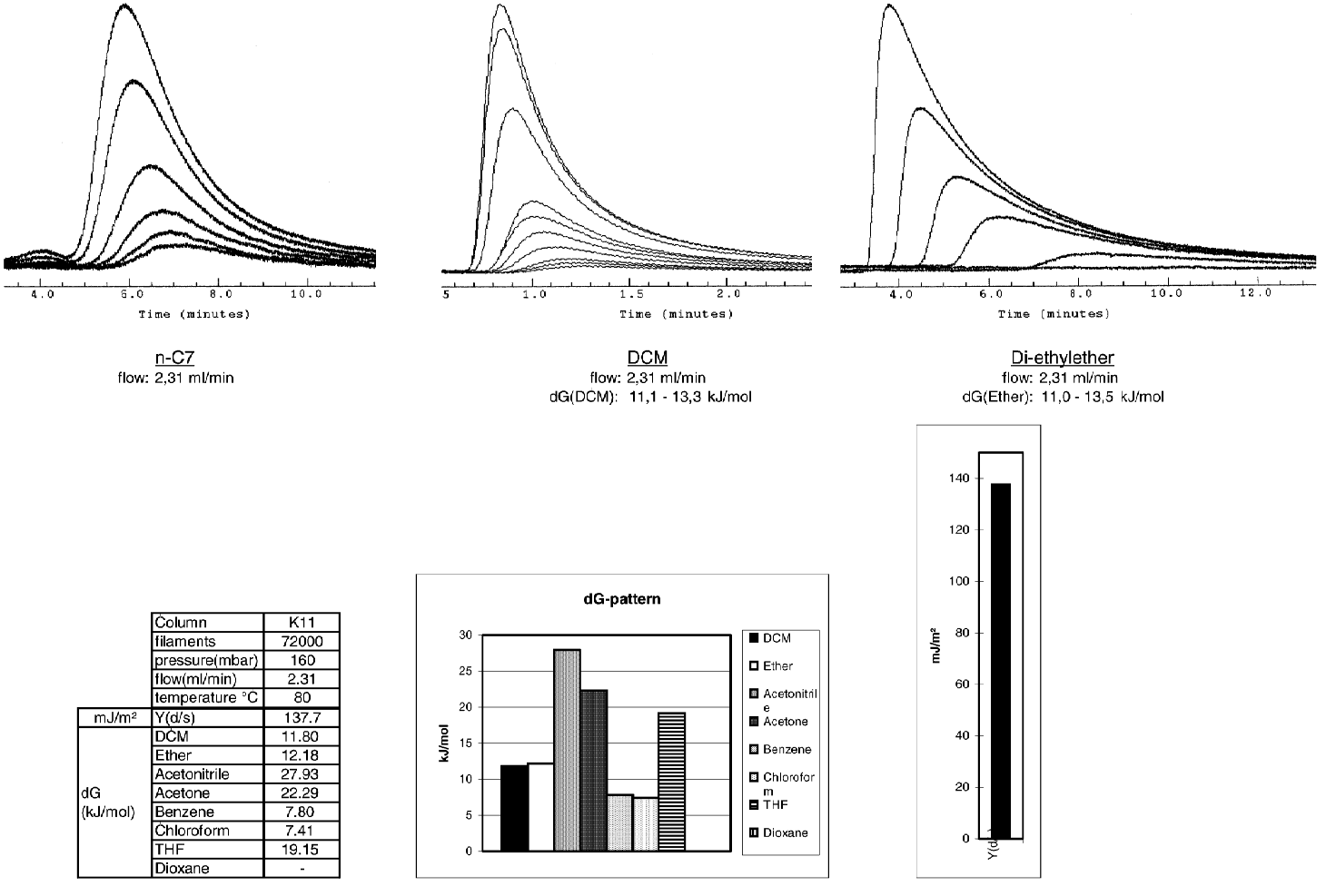

	Column	K11
	filaments	72000
	pressure(mbar)	160
	flow(ml/min)	2.31
	temperature °C	80
mJ/m²	Y(d/s)	137.7
dG (kJ/mol)	DCM	11.80
	Ether	12.18
	Acetonitrile	27.93
	Acetone	22.29
	Benzene	7.80
	Chloroform	7.41
	THF	19.15
	Dioxane	-

Fig. 13. IGC data chart of Carbon fiber TEN4 (with surface treatment; see legend of Fig. 12 for experimental details).

explanation could be that the extraction removes some apolar and involatile contaminants which remain on the fiber surface during the thermal conditioning of the IGC column. Both the standard and epoxy finish clearly affect the surface characteristics of Twaron. The Twaron surface itself is amphoteric–acidic while after application of the finishes the surface becomes more basic. The interaction with the basic probes decreases while the interaction with the acidic probes increases when the finishes are applied. The results indicate that the standard finish is completely removed by the Soxhlett extraction. After the ethanol extraction the IGC data is almost identical to those of the bare fiber. On the other hand the new epoxide finish cannot be removed by the ethanol extraction as it is a crosslinked phase. This is indeed also confirmed by the IGC analysis.

5. Conclusions

IGC can be a valuable tool for the characterization of fiber surfaces. This technique can also be applied as a screening tool for industrial fibers. An efficient IGC measurement scheme was developed on the basis of the dispersive component of the surface energy, Gibbs energy of acid–base interaction and surface energy heterogeneity to reduce the IGC analysis time to a couple of hours per sample.

Too high values for the dispersive component of the surface energy are obtained when the adsorption area occupied by a single adsorbed *n*-alkane probe molecule is estimated from parameters of the corresponding liquid. Comparable values are obtained when the area per methylene unit (Doris–Gray method) or measured probe areas are employed.

For the fibers studied in this work meaningful Gibbs energy values of the acid–base interaction were only obtained with the polarizability concept of Donnet and coworkers. The use of surface tension, boiling point, or vapor pressure of the polar and apolar probes often lead to negative acid–base interaction energies. From the temperature dependence of the Gibb's acid–base interaction energy accurate enthalpy data could be obtained. However, no clear relationship between the enthalpy of acid–base interaction and the acceptor and donor numbers of the probes could be established. Consequently, no meaningful acid–base surface parameters could be obtained.

The enhanced interaction measured for some polar probes on activated carbon fibers at very low probe loadings is probably related to the heterogeneity of the interaction energy of the active sites at the surface. The corresponding adsorption isotherm is curved at low probe concentrations and becomes linear at higher concentrations. Surface activation of carbon fibers usually invokes stronger concentration effects of basic probes. Therefore, it can be concluded that due to these surface treatments a limited number of very active acidic sites are generated.

Acknowledgements

Dr B. Wohlmann from Tenax Carbon fibers is gratefully acknowledged for supplying the various carbon fiber samples and for fruitful discussions. The IGC analysis of the Twaron fibers was made possible by Dr. J. Mahy from Akzo Nobel and Dr P. de Lange from Acordis (former Akzo Nobel Fibers). Finally, acknowledgments are due to Prof. Dr H. Poppe and Prof. Dr R. Tijssen from the University of Amsterdam for critical evaluation of this work.

References

[1] A.V. Kiselev, in: J.C. Giddings, R.A. Keller (Eds.), Advances in Chromatography, Marcel Dekker, New York, 1967.
[2] J.R. Condor, C.L. Young, Physiochemical Applications of Gas Chromatography, Wiley, New York, 1979.
[3] A. Voelkel, Crit. Rev. Anal. Chem. 22 (1991) 411.
[4] D.R. Lloyd, T.C. Ward, H.P. Schreiber (Eds.), Inverse Gas Chromatography, ASC Symposium Series, Vol. 391, American Chemical Society, Washington DC, 1989.
[5] J. Schultz, L. Lavielle, Inverse Gas Chromatography, in: D.R. Lloyd, T.C. Ward, H.P. Schreiber (Eds.), ASC Symposium Series, Vol. 391, American Chemical Society, Washington DC, 1989, Chapter 14.
[6] A.E. Bolvari, T.C. Ward, Inverse Gas Chromatography, in: D.R. Lloyd, T.C. Ward, H.P. Schreiber (Eds.), ASC Symposium Series, Vol. 391, American Chemical Society, Washington DC, 1989, Chapter 16.
[7] J. Schultz, L. Lavielle, C. Martin, J. Adhesion 23 (1987) 45.
[8] H.-J. Jacobasch, K. Grundle, P. Uhlmann, F. Simon, E. Mader, Composite Interf. 3 (1996) 293.

[9] D.W. Dwight, F.M. Fowkes, D.A. Cole, M.J. Kulp, P.J. Sabat, L. Salvati Jr., T.C. Huang, J. Adhesion Sci. Technol. 4 (1990) 619.
[10] E. Papirer, H. Balard, J. Adhesion Sci. Technol. 4 (1990) 357.
[11] J. Felix, P. Gatenholm, H.P. Schreiber, J. Appl. Polym. Sci. 51 (1994) 285.
[12] R.S. Farinato, S.S. Kaminski, J.L. Courter, J. Adhesion Sci. Technol. 4 (1990) 633.
[13] B.J. Briscoe, P.R. Williams, J. Adhesion Sci. Technol. 5 (1991) 23.
[14] S.P. Wesson, R.E. Allred, in: D.R. Lloyd, T.C. Ward, H.P. Schreiber (Eds.), Inverse Gas Chromatography, ASC Symposium Series, Vol. 391, American Chemical Society, Washington DC, 1989, Chapter 15.
[15] A.B. Garcia, A. Cuesta, M.A. Montes-Moran, A. Martinez-Alonso, J.M.D. Tascon, J. Colloid Interf. Sci. 192 (1997) 363.
[16] F. Simon, H.-J. Jacobasch, D. Pleul, P. Uhlmann, Progr. Colloid Polym. Sci. 101 (1996) 184.
[17] M.N. Belgacem, G. Czereminszkin, S. Sapieha, A. Gandini, Cellulose 2 (1995) 145.
[18] B. Riedl, P.D. Kamden, J. Adhesion Sci. Technol. 6 (1992) 1053.
[19] W. Shen, I.H. Parker, Y.J. Sheng, J. Adhesion Sci. Technol. 12 (1998) 161.
[20] M.A. Tshabalala, J. Appl. Polym. Sci. 65 (1997) 1013.
[21] C.S. Flour, E. Papirer, J. Colloid Interf. Sci. 91 (1983) 69.
[22] E. Osmont, H.P. Schreiber, in: D.R. Lloyd, T.C. Ward, H.P. Schreiber (Eds.), Inverse Gas Chromatography, ASC Symposium Series, Vol. 391, American Chemical Society, Washington DC, 1989, Chapter 17.
[23] M.L. Tate, Y.K. Kamath, S.P. Wesson, S.B. Ruetsch, J. Colloid Interf. Sci. 177 (1996) 579.
[24] H.-J. Jacobach, I. Grosse, Fibres and Textiles in Eastern Europe (1996) 66, Jan/March.
[25] A.J. Vukov, D.G. Gray, in: D.R. Lloyd, T.C. Ward, H.P. Schreiber (Eds.), Inverse Gas Chromatography, ASC Symposium Series, Vol. 391, American Chemical Society, Washington DC, 1989, Chapter 13.
[26] G.M. Dorris, D.G. Gray, J. Colloid Interf. Sci. 71 (1979) 93.
[27] G.M. Dorris, D.G. Gray, J. Colloid Interf. Sci. 77 (1980) 355.
[28] P.N. Jacob, J.C. Berg, Langmuir 10 (1994) 3086.
[29] P. Mukhopadhyay, H.P. Schreiber, Colloids Surf. A 100 (1995) 47.
[30] U. Panzer, H.P. Schreiber, Macromolecules 25 (1992) 3633.
[31] C.R. Hegedus, I.L. Kamel, J. Coatings Technol. 65 (1993) 23.
[32] F.M. Fowkes, Ind. Eng. Chem. 56 (1964) 40.
[33] F.M. Fowkes, J. Adhesion 4 (1972) 152.
[34] F.M. Fowkes, M.A. Mostafa, Ind. Eng. Chem., Prod. Res. Dev. 17 (1978) 3.
[35] F.L. Riddle, F.M. Fowkes, J. Am. Chem. Soc. 112 (1990) 3258.
[36] V. Gutmann, The Donor Acceptor Approach To Molecular Interactions, Plenum Press, New York, 1978.
[37] M. Nardin, E. Papirer, J. Colloid Interf. Sci. 137 (1990) 534.
[38] D.J. Brookman, D.T. Sawyer, Anal. Chem. 40 (1968) 106.
[39] S. Dong, M. Brendle, J.B. Donnet, Chromatographia 28 (1989) 469.
[40] J.B. Donnet, S.J. Park, H. Balard, Chromatographia 31 (1991) 435.
[41] T. Tamieh, M. Nardin, M. Rageui-Lescourt, H. Haidara, J. Schultz, Colloids Surf. A 125 (1997) 155.
[42] K.U. Gross, J. Colloid Interf. Sci. 190 (1997) 241.
[43] W.D. Bascom, R.M. Jensen, J. Adhesion 19 (1986) 219.
[44] S.J. Park, J.P. Donnet, J. Colloid Interf. Sci. 200 (1998) 46.
[45] H. Balard, A. Saada, J. Hartmann, D. Aouadj, E. Papirer, Macromol. Symp. 108 (1996) 63.
[46] M. Fafard, M. El-Kindi, H.P. Schreiber, G. Dipaola-Baranyi, A.M. Hor, J. Adhesion Sci. Technol. 8 (1994) 1383.
[47] M. Pyda, G. Guiochon, Langmuir 13 (1997) 1020.
[48] J. Jagiello, G. Ligner, E. Papirer, J. Colloid Interf. Sci 137 (1990) 128.
[49] H. Balard, A. Saada, E. Papirer, B. Siffert, Langmuir 13 (1997) 1256.
[50] J.F.K. Huber, R.G. Gerritse, J. Chromatogr. 58 (1971) 137.
[51] T. Paryjczak, Gas Chromatography in Adsorption and Catalysis, Ellis Horwood Limited, West Sussex, UK, 1986.
[52] S.J. Park, J.P. Donnet, J. Colloid Interf. Sci. 206 (1998) 29.